ACS APPLIED POLYMER MATERIALS

pubs.acs.org/acsapm

Article

# Blending or Bonding? Mechanochromism of an Aggregachromic Mechanophore in a Thermoplastic Elastomer

Cosimo Micheletti, Valentina Antonia Dini, Marco Carlotti, Francesco Fuso, Damiano Genovese, Nelsi Zaccheroni, Chiara Gualandi, and Andrea Pucci*

Cite This: *ACS Appl. Polym. Mater.* 2023, 5, 1545−1555

Read Online

ACCESS | Metrics & More | Article Recommendations | Supporting Information

**ABSTRACT:** A straightforward way for the preparation of mechanochromic polymers consists of incorporating a suitable content of a mechanophore in the polymeric matrix either by physical dispersion or *via* covalent functionalization. Although covalent incorporation may require demanding chemical efforts, this approach can offer significant advantages over physical dispersion. In this work, a common thermoplastic elastomer, styrene-*b*-(ethylene-*co*-butylene)-*b*-styrene triblock copolymer grafted with maleic anhydride (SEBS-MAH), was covalently functionalized with 1-aminomethylpyrene (AMP). MAH functional groups are covalently linked to the ethylene-*co*-butylene blocks, thus allowing a precise and selective confinement of the chromogenic AMP units in the soft block. Flat, fully conjugated pyrene units undergo the reversible formation of $\pi-\pi$ aggregates, readily distinguishable by their red-shifted emission. These aggregates were heavily affected by the application of mechanical stimuli. Despite the low degree of mechanophore functionalization (about 1 wt %), uniaxial deformation of the polymer was reliably monitored *via* fluorescence and a clear drop in the excimer to monomer emission ratio ($I_E/I_M$) was observed starting from 50% of strain. The marked mechanochromism was confirmed by emission lifetime measurements and also by near-field investigations. In addition, the mechanoresponse showed good reversibility after repeated stress−relaxation cycles. Control experiments performed on formulations comprising a physical dispersion of pyrene in unfunctionalized SEBS showed faint excimer emission and a negligible mechanochromic response up to 5 wt % of doping, in substantial agreement with the scanning near-field optical microscopy analysis. An evident drop of the $I_E/I_M$ ratio occurred for 10 wt % of pyrene, albeit the excimer emission remained predominant even at the highest deformation, being a smaller fraction of pyrene moieties involved. Overall, the covalent approach appeared as an elegant procedure to confine the chromogenic unit in the soft phase of block copolymers and thus to provide an elastomeric film showing a detectable and reversible mechanochromic response with a modest (i.e., ∼1 wt %) amount of pyrene molecules, i.e., 10 times smaller compared to the dispersed system.

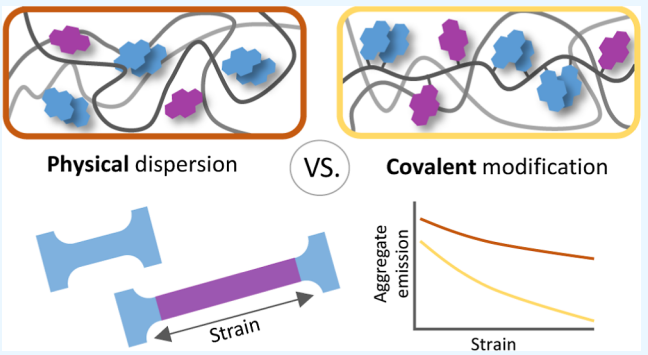


**KEYWORDS:** *pyrene, styrene-block copolymers, physical mixing, covalent bonding, chromogenic polymers, mechanochromism*



## 1. INTRODUCTION

Excessive mechanical stress in polymeric materials can lead to the breakage of the macromolecular chains,[1−3] which may induce degradation and macroscopic failures.[4] The reliable monitoring of the strain is a powerful tool to prevent premature and potentially disabling damage.[5] In this context, mechanochromic polymers and composites that can change their optical properties under mechanical stimuli have attracted ever-increasing attention.[6−14] Moreover, the real-time measurement of optical variations allows for an easily accessible and immediate readout of the forces at play without the need for any electronic apparatus.

In most cases, mechanochromic materials rely on the presence of mechanophores in the polymeric matrix—, i.e., units capable of changing their absorption and/or emission properties upon mechanical stress. The mechanophore can be either covalently linked to the main chains or finely dispersed in the bulk. The mechanochromic response can be based on the rupture of covalent bonds or of non-covalent interactions. Examples of the first type of mechanophores include spiropyranes,[15−18] 1,2-dioxetanes,[19−22] diacetylenes, and diarylbibenzofuranones.[23−25] Being the mechanoactivation based on the rupture of a covalent bond, they typically have a poor response in the low-strain regime of deformation. Their deactivation is generally slow; in many cases, the bond rupture is irreversible, and, in some cases,

Received: November 24, 2022
Accepted: January 17, 2023
Published: January 26, 2023

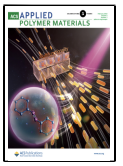

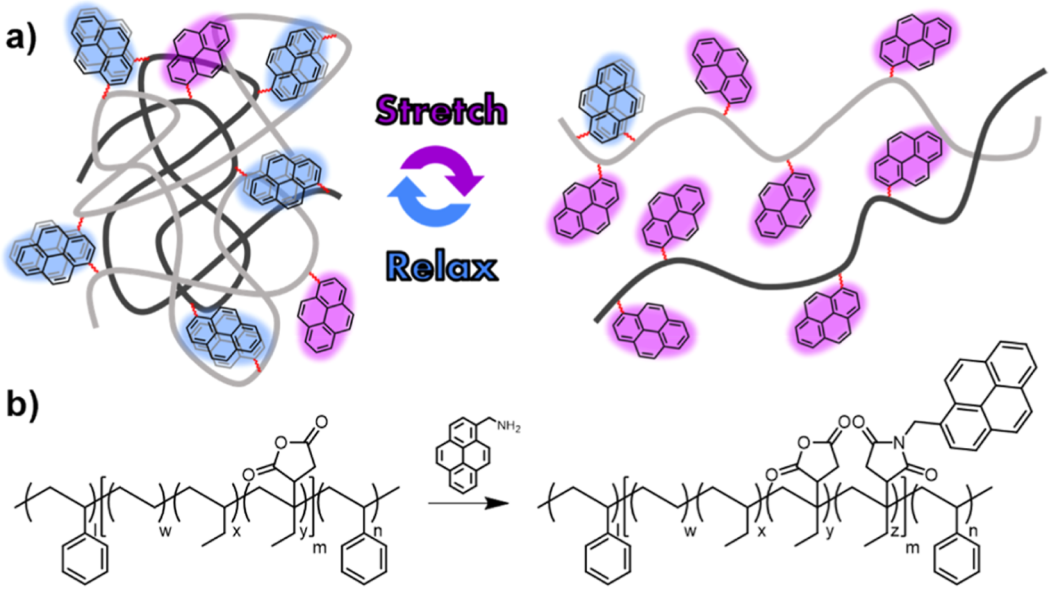


**Figure 1.** (a) Schematic representation of the AMP-functionalized SEBS: when no stress is applied, the emission of the material is dominated by the excimer. The deformation causes the gradual breaking of the excimer aggregates leading to the increase of the monomer emission; (b) covalent functionalization of SEBS-MAH with AMP.

other stimuli (such as heat or light) could interfere with the readout. These features can limit their utility.

The second type of mechanophores comprises supramolecular dye-host assemblies and non-covalent aggregates (aggregachromic mechanophores), which can disassemble and break in response to the shear forces that arise in the polymer matrix upon mechanical stress. Depending on the dye's self-assembling characteristics and affinity for the dispersing media, such mechanophores may aggregate above a certain concentration showing optical properties that differ from those of the isolated monomer; the mechanical stimulus leads to aggregate breakdown, and a change in the optical proprieties is consequently observed.[26−28]

Among "non-covalent probes", excimer-forming fluorophores are particularly interesting.[27−38] These fluorophores typically form dimers in solution only at the excited state, but when in reduced mobility conditions, such as when embedded in a polymer matrix, they may undergo dimer or aggregate formation even at the ground state. In these cases, dimers may be considered as the edge of aggregachromic mechanophores, representing in principle the smallest possible aggregate made of only two molecular moieties. When no stress is applied, the emission of the material is dominated by the excimer. The deformation causes the gradual breaking of the excimer aggregates leading to an increase in the monomer emission. In this frame, different scientists have reported elegant results, such as Weder et al. discussing mechanochromic polymer containing cyano-oligo(*p*-phenylene vinylene) dispersed in polyethylene[38,39] or Ruggeri et al. describing blends of linear low-density polyethylene and perylene tetracarboxylic acid bis-imides containing linear or branched alkyl chains.[28] Nevertheless, one can find in the literature only a few examples in which the excimer-forming probe is covalently linked to the polymer. This approach is appealing as it may lead to a more uniform distribution of the fluorophores in the polymer and is expected to improve the transduction from the external stimulus to the mechanoresponse. Examples of this approach include excimer-forming cyano-substituted oligo(*p*-phenylene vinylene) dyes which were first blended[37] and later covalently incorporated[40] into the backbone of polyurethanes by Weder's research group. Among the common excimer-forming probes, pyrene was successfully incorporated into the polymer backbone or employed as a cross-linker to obtain materials with a reversible mechanochromic response.[41−44] Recently, Dalcanale et al. obtained mechanoresponsive materials based on high-density and very low-density polyethylene grafted with maleic anhydride (MAH) functionalized with 1-aminopyrene *via* reactive extrusion.[45]

In this study, we describe the fabrication and characterization of a mechanochromic thermoplastic elastomer covalently functionalized with pyrene moieties (Figure 1a) and compare its chromogenic response with that of a physically mixed blend, including analogue fluorophores. As a thermoplastic elastomer potentially capable of reversible mechanochromism, a styrene-*b*-(ethylene-*co*-butylene)-*b*-styrene triblock copolymer (SEBS) was selected. This material offers several advantages, such as a low Young's modulus, excellent processability, and good chemical and UV resistance, making it suitable for both indoor and outdoor applications. We employed a commercially available SEBS grafted with MAH (SEBS-MAH) to allow for a simple functionalization procedure (Figure 1b). We chose 1-aminomethylpyrene (AMP) as a pyrenic derivative since it can readily react with the anhydride grafted to the polymer chains, and its aggregachromic properties, characterized by efficient excimer formation, are well-known. In the selected matrix, the functionalization with the pyrene moieties were of interest to only the soft domains of ethylene−butylene. The mechanochromic response is evaluated in terms of sensitivity and reversibility, and it is compared with that of blended samples obtained with a similar polymeric matrix without grafted MAHs (SEBS), in which pyrene could be potentially dissolved in both blocks.

## 2. EXPERIMENTAL SECTION

**2.1. Materials.** Tetrahydrofuran (THF), toluene, methanol (MeOH), deuterated dimethyl sulfoxide (DMSO-$d_6$), AMP hydro-



https://doi.org/10.1021/acsapm.2c02037
ACS Appl. Polym. Mater. 2023, 5, 1545−1555

chloride (AMP-Cl, 95%), pyrene (98%), and ammonium hydroxide aqueous solution (25%) were obtained from Sigma-Aldrich (Germany) and used as received. SEBS functionalized on the aliphatic segment with MAH (SEBS-MAH, 1 wt % of grafted anhydrides) was kindly provided by Auser Polimeri S.R.L. (Italy). The product exhibits a degree of functionalization of grafted anhydride equal to 1 wt %, a percentage of styrene of 28 mol %, an amount of residual unsaturation below 3%, and a density equal to 0.919 g $cm^{-3}$. SEBS used in this work (SEBS YH-501) was supplied by Sinopec (China) in the form of a white powder. The product has a linear structure and consists of 30 mol % of styrene units. Both SEBS and SEBS-MAH were purified by dissolution in toluene and reprecipitation in MeOH (toluene/MeOH = 1:20 v/v). The polymer was recovered by filtration and dried under vacuum. After purification, SEBS-MAH was dried for 4 h at 170 °C under vacuum to convert all carboxylic acid groups, formed upon hydrolysis, back to anhydrides. Thermal treatment was monitored by Fourier-transform infrared (FT-IR) in attenuated total reflection (ATR) mode (Figure S4).

**2.2. Converting AMP-Cl to AMP.** AMP-Cl (0.43 g, 1.5 mmol) was dissolved in MeOH (35 mL), and $NH_4OH$ (40 mL) was added. A color change from yellow to colorless was observed (Figure S1). The day after, AMP was recovered by filtration (white solid), washed with cold methanol, and dried under vacuum. 0.28 g was recovered (1.2 mmol, yield 80%). AMP was utilized without further purification. AMP was characterized by $^1$H NMR in DMSO-$d_6$ and by FT-IR in ATR mode (Figures S2 and S3).

$^1$H NMR (500 MHz, DMSO-$d_6$, 25 °C) $\delta$: 8.42 (d, $J$ = 9.2 Hz, 1H), 8.32−8.24 (m, 3H), 8.21 (d, $J$ = 9.2 Hz, 1H), 8.19−8.10 (m, 3H), 8.06 (t, $J$ = 7.6 Hz, 1H), 4.47 (s, 2H), 2.08 (s, 2H).

FT-IR (ATR) $cm^{-1}$: 3365, 3306, 3038, 2917, 2890, 2851, 1603, 1587, 1488, 1451, 1432, 1415, 1314, 1282, 1185, 1069, 886, 842, 818, 811, 791, 762, 723, 712, 680.

**2.3. Preparation of SEBS-AMP and UV−Vis Analysis to Determine the Grafting Extent.** 4.84 g of SEBS-MAH (0.45 mmol of grafted anhydrides) was dissolved in dry THF (30 mL). Then, 64 mg of AMP (0.28 mmol, 0.6 equiv) was added, and the reaction was carried out at reflux for 48 h under stirring. The polymer was precipitated in MeOH (THF/MeOH = 1:20 v/v) and recovered by filtration (4.24 g). To remove the unreacted AMP, the crude product was purified by Kumagawa extraction in MeOH for 48 h and then dried under vacuum. The extent of the reaction was monitored by FT-IR in ATR mode (Figure S5) by observing the disappearance of the peaks at 1866 and 1788 $cm^{-1}$ ($\nu_{C=O}$ of anhydride) and the appearance of the peak at 1711 $cm^{-1}$ ($\nu_{C=O}$ of imide). To determine the degree of functionalization, UV−vis spectroscopy was employed. First of all, a calibration curve was obtained by plotting the absorbance at 345 nm of stock solutions of AMP in toluene. The range of concentration spanned between $6.1 \times 10^{-6}$ and $3.1 \times 10^{-5}$ M, corresponding to absorbances in the range of 0.2−1.1 (Figure S6). A solution of SEBS-AMP (0.51 mg $mL^{-1}$) in toluene was prepared, and the degree of functionalization with respect to the grafted anhydride (85.6%) and the weight percentage of grafted pyrene unit were calculated (1.1 wt %).

**2.4. Preparation of Blends of Pyrene in SEBS.** 1.00 g of SEBS was dissolved in 50 mL of toluene, then the proper amount of pyrene (1−10 wt %) was added, and the solution was left under stirring overnight. The solvent was removed under vacuum, and the polymer was recovered.

**2.5. Film Preparation.** About 1.0 g of pelletized pyrene in SEBS (SEBS-P) or SEBS-AMP was pressed twice for 5 min at 150 °C and 150−200 bar. Before compression, the polymer was allowed to soften between the hot plates for 2 min.

**2.6. Characterization.** $^1$H NMR spectra were carried out at room temperature and recorded on a JEOL spectrometer operating at 500 MHz and using 5 mm tubes and by setting 32 scans. The residual solvent peak was employed as an internal standard.

FT-IR spectra were acquired by a Nicolet iS50 spectrometer (Thermo Fisher). The samples were analyzed in the ATR mode in the spectral range between 4000 and 600 $cm^{-1}$ by setting 32 or 64 scans and a resolution of 4 $cm^{-1}$. The ATR accessory (ATR ITX) contained a diamond crystal (by employing this crystal, the penetration of infrared radiation is about 2 $\mu$m at wavelength numbers 1000 $cm^{-1}$) at a nominal incident angle of 45°.

UV−vis absorption spectroscopy was performed using a Cary 5000 UV−vis−NIR spectrophotometer (Agilent).

Fluorescence spectra were acquired on a Horiba Jobin−Yvon Fluorolog-3 spectrofluorometer equipped with a 450 W xenon arc lamp, double-grating excitation, and single-grating emission monochromator. The selected excitation wavelengths were close to the absorption peak at longer wavelengths. For polymeric films, the samples were rotated 30° with respect to the excitation beam, and the detector was set in the front-face mode.

An Edinburgh FLS920 fluorometer equipped with a photomultiplier Hamamatsu R928P and connected to a PCS900 PC card was used for the fluorescence lifetime measurements based on the time-correlated single photon counting technique.

Scanning near-field optical microscopy (SNOM) in the emission mode was carried out with a custom-made apparatus, making use of a tapered and apertured optical fiber (LovaLite, 50 nm apical aperture) coupled with a 365 nm light-emitting diode (LED) (ThorLabs M365) as the near-field probe. Fluorescence emission, collected in the far field at 45° off-normal by a long working distance microscope objective (Mitutoyo 10× Plan Apo), was spectrally analyzed by interference filters (CVI Laser Optics) and detected by miniaturized photomultipliers (Hamamatsu R9880U-01). A sketch of the experimental configuration is shown in Figure S14. Amplitude modulation of the LED radiation and lock-in demodulation of the signal (Stanford Research SR830DSP) were used to improve the signal-to-noise ratio.

Differential scanning calorimetry (DSC) analyses were performed with a TA Instruments Discovery DSC 250 calorimeter. About 9 mg of polymer film obtained by compression molding was put in a 3 mm aluminum Tzero Pan plugged with a Tzero hermetic lid. The samples were analyzed according to the following cycle: heating from RT to 150 °C at 10 °C $min^{-1}$; cooling from 150 to −90 °C at 10 °C $min^{-1}$; and a second heating scan to 150 °C at 10 °C $min^{-1}$. An isotherm of 5 min was set between each heating−cooling scan.

Stress−strain analyses were performed on Tinius Olsen H10KT equipped with a 500 N load cell, using an extension rate of 10 mm $min^{-1}$. Dog-bone specimens with a gauge length of 20 mm and a width of 5 mm were used. Three replicates were analyzed for each sample, and the results are given in terms of mean and standard deviation. The thickness was measured for each sample using a microcaliper.

## 3. RESULTS AND DISCUSSION

**3.1. Preparation and Characterization of SEBS-Based Mechanochromic Systems.** We selected AMP as a fluorophore because of the suitable and rich photophysical properties of the pyrene core, together with its optimal thermal and chemical stability. In particular, the two fluorescence emissions of pyrene, as a monomer and as an excimer, are characterized by a large spectral separation and high luminescence quantum yields, with long lifetimes of the excited states that are also affected by oxygen concentration.[46,47] Pyrene-functionalized SEBS (SEBS-AMP) was synthesized starting from a SEBS-MAH, exploiting its straightforward reaction with the amino groups of AMP forming a robust succinimide (Figure 1b).[48,49] The proceeding of the reaction was easily monitored *via* FT-IR spectroscopy thanks to the disappearance of the absorption bands around 1788 $cm^{-1}$ (strong) and 1866 $cm^{-1}$ (weak), which are characteristic of saturated cyclic anhydrides (originating from the anti-symmetric and symmetric C=O stretching vibration, respectively),[50−52] and the formation of a signal around 1711 $cm^{-1}$, ascribable to the imide formation (Figure S5). The absence of NH stretching at 1530 and 1650 $cm^{-1}$ excludes the formation of amide derivatives.[52] The obtained SEBS-AMP was purified by Kumagawa extraction to ensure the complete removal of


https://doi.org/10.1021/acsapm.2c02037
ACS Appl. Polym. Mater. 2023, 5, 1545−1555

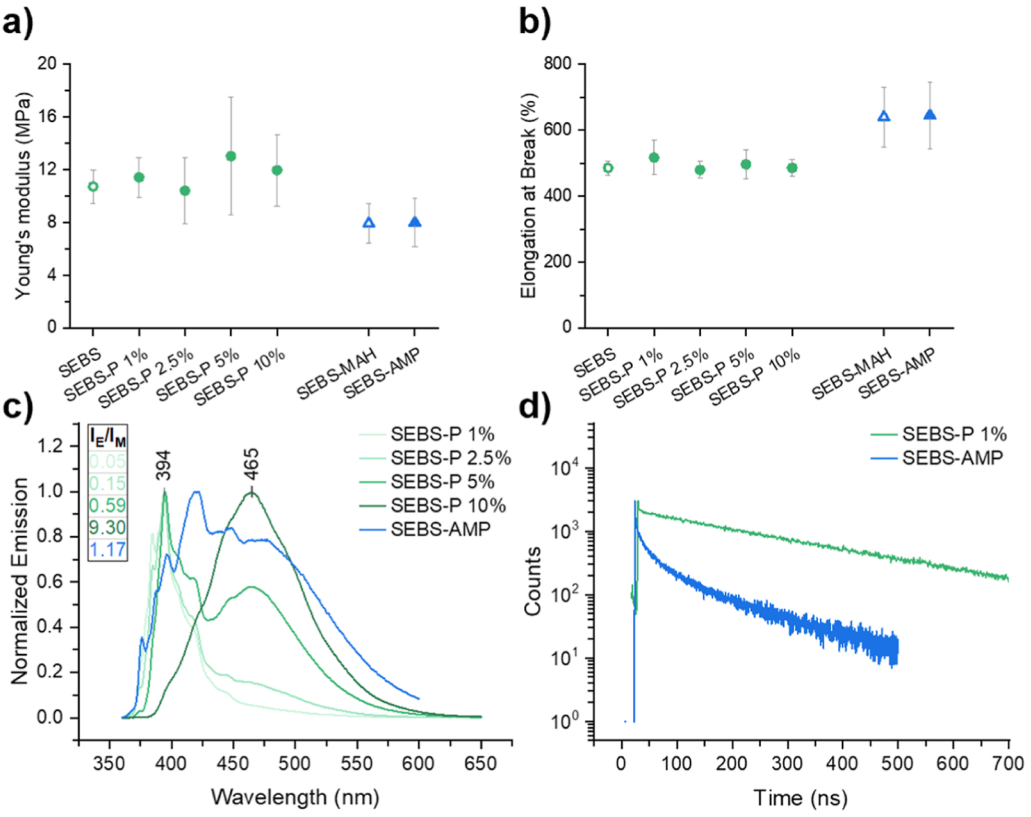


**Figure 2.** Young's moduli (a) and elongation at break (b) for the pristine polymeric matrices (empty symbols) and for functionalized/dispersed samples (filled symbols); three replicates were performed for each sample and the result is reported as mean ± SD; (c) normalized emission spectra $\lambda_{exc}$ = 345 nm of SEBS-P with different amounts of dispersed pyrene and SEBS-AMP; and (d) lifetimes of monomeric emission $\lambda_{em}$ = 394 nm in SEBS-P 1% and SEBS-AMP.

unreacted pyrene, and the weight percentage of grafted pyrene was calculated to be 1.1 wt % by UV−vis analysis (Figure S6).

We also prepared blend samples of unfunctionalized SEBS and pyrene by physical dispersion (SEBS-P) in order to compare the optical and mechanical properties of the covalently functionalized matrix to those of dispersed samples. In this latter case, pyrene was introduced, ranging from 1 to 10 wt %. Films were prepared by hot compression molding. The UV−vis spectra of the SEBS-P and SEBS-AMP films (Figure S7 as an example) showed a slight bathochromic shift of 2 nm as well as a broadening of the absorption bands with respect to toluene solutions (Figure S6), thus suggesting the occurrence of pyrene preassociation or ground state excimer formation in the polymer environment.[46] This behavior was confirmed from the ratio Pa of the absorption intensity of the most intense band to that of the adjacent minimum at shorter wavelength, which decreased from 2.5 in the toluene solution to 1.9 in the case of the SEBS-AMP film.

Tensile stress−strain tests and DSC, before and after the introduction of the fluorophore, are reported in the Supporting Information (Figures S8 and S9 and Table S1). Young's modulus and deformation at break are shown in Figure 2a,b. These characterizations assessed that thermal and mechanical properties of covalently functionalized, blend samples and pristine polymers were almost identical, thus demonstrating that functionalization and dispersion processes do not substantially affect the polymer thermomechanical properties.

**3.2. SEBS-P and SEBS-AMP Fluorescence Characterization.** The amount of excimer in covalently functionalized (SEBS-AMP) and blend samples (SEBS-P) was assessed by fluorescence emission spectroscopy (Figure 2c). In particular, we calculated the excimer to monomer emission ratio at their maxima, 465 and 394 nm, respectively ($I_E/I_M$). In the case of SEBS-P systems, the sample containing the lowest amount of pyrene (1 wt %) showed poor excimer formation ($I_E/I_M$ < 0.1, Figure S10). The presence of excimer started to be evident from 2.5% of dispersed pyrene (although with low intensity, $I_E/I_M$ = 0.15, Figure S11) and grew on reaching 5% ($I_E/I_M$ = 0.59) and 10% ($I_E/I_M$ = 9.30). In the latter sample, a pronounced broad peak around 465 nm is evident, while the emission from monomeric species was negligible. Remarkably, the covalently functionalized sample showed an evident excimer band ($I_E/I_M$ = 1.17) despite comprising only 1 wt % of pyrene functionalities. In this sense, we can estimate the $I_E/I_M$ for SEBS-AMP to be about 23 times larger than the SEBS-P 1% sample doped with the same amount of pyrene (and even about 2 times larger than SEBS-P 5%), thus indicating the higher tendency of pyrene moieties to form fluorescent aggregates in the covalently functionalized SEBS-AMP system compared to the dispersed system.

This observation can be partially explained considering that, in the covalently linked sample, the functionalization interests only the ethylene−butylene soft block of the polymeric matrix, while in the blend samples, the fluorophores are dispersed throughout the polymeric matrix (including the styrene hard block). Therefore, in the SEBS-AMP system, the pyrene units are, on average, closer to each other and the formation of excimers and aggregates is enhanced. This hypothesis is also confirmed by the larger $I_E/I_M$ ratio shown by the SEBS-AMP system compared to that reported by Dalcanale et al. for pyrene-


https://doi.org/10.1021/acsapm.2c02037
ACS Appl. Polym. Mater. 2023, 5, 1545−1555

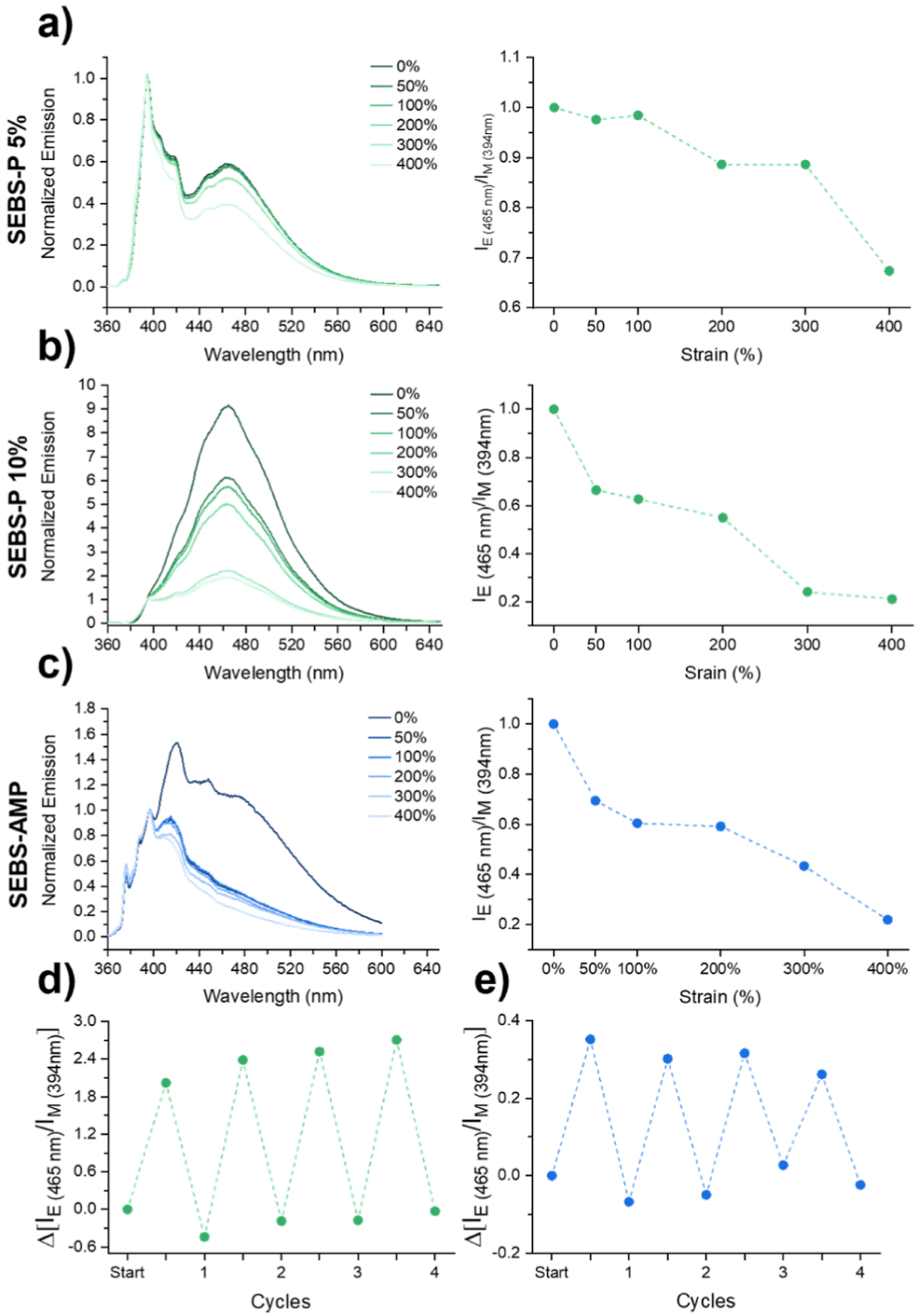


**Figure 3.** Emission ($\lambda_{exc}$ = 345 nm, normalized at 396 nm) and normalized $I_E/I_M$ for SEBS-P 5% (a), SEBS-P 10% (b), and SEBS-AMP (c) at different strains; variation of the excimer to monomer intensity ratio, $\Delta(I_E/I_M) = (I_E/I_M)_{start} - (I_E/I_M)_{400\%}$, under uniaxial loading and unloading cycles for SEBS-P 10% (d) and SEBS-AMP (e).

grafted polyethylene containing similar pyrene concentration.[45] The confinement of the chromogenic probe into one single domain allows the formation of the excimer band at lower dye contents.

Consistently, the monomer emission had a shorter lifetime (Figure 2d) in SEBS-AMP than in SEBS-P 1%, in agreement with the most extensive excimer band observed in the emission spectra of SEBS-AMP:[53] the monomeric emission lifetime of SEBS-AMP is shorter because a larger fraction of the excited



https://doi.org/10.1021/acsapm.2c02037
ACS Appl. Polym. Mater. 2023, 5, 1545−1555

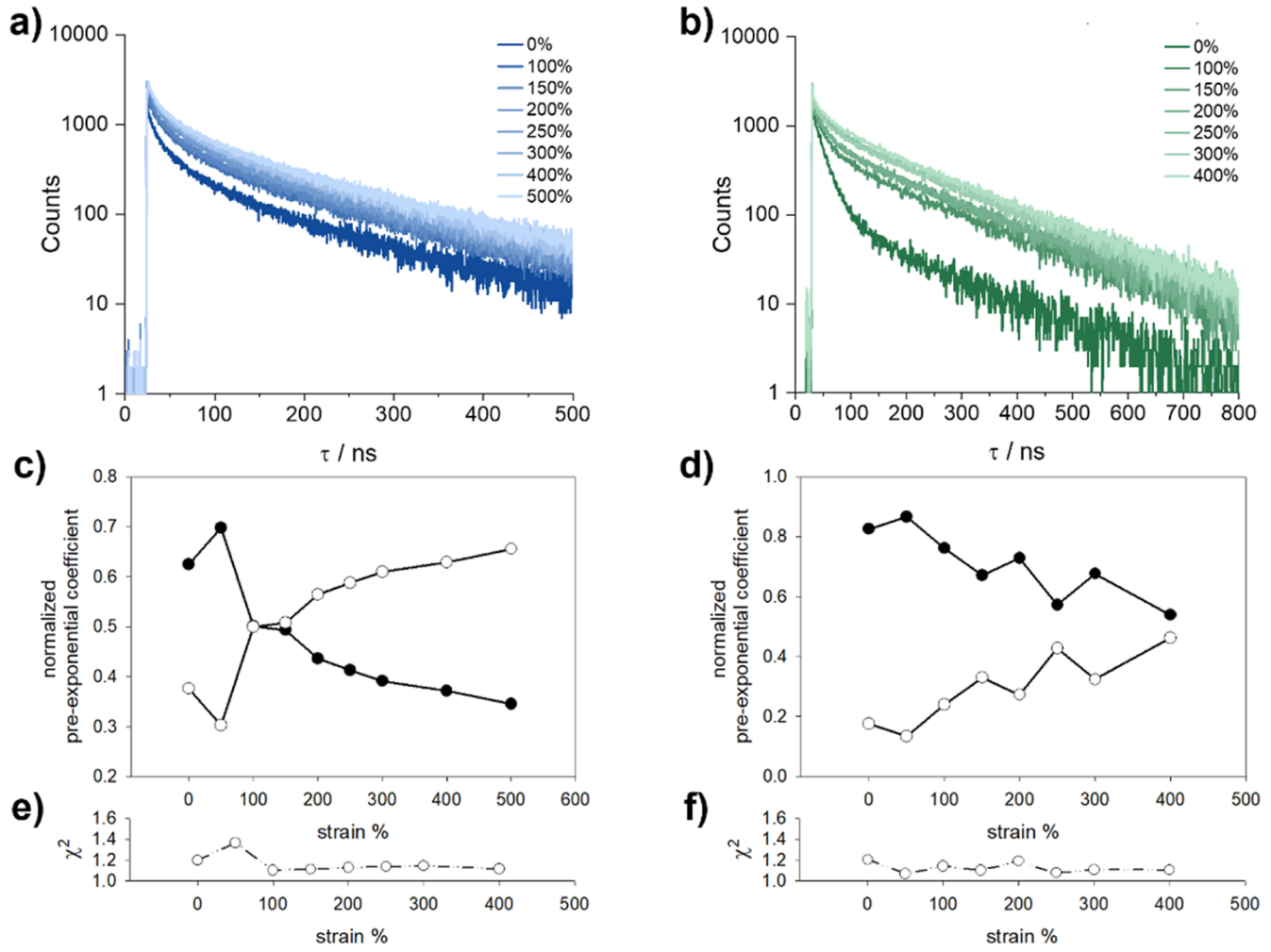


**Figure 4.** Emission decays of SEBS-AMP (a) and SEBS-pyrene 10% (b); (c,d) pre-exponential factors obtained with a fixed lifetime, three-exponential decay fittings of data shown in (a,b), respectively. B1 (solid circles) represents the fraction of quenched pyrenes (excimer forming pyrene moieties), while B2 + B3 (hollow circles) represents the fraction of unquenched pyrenes (non-excimer forming moieties); $\chi^2$ (e,f) of the fittings is also reported as an indication of the good quality of the fitting.

states of pyrenes leads to either formation of excimers or to the excited state of aggregates, which are responsible for the red-shifted emission at 465 nm.

We then characterized the fluorescent behavior of these systems under uniaxial deformation. SEBS-P with 1 and 2.5 wt % of dispersed pyrene showed only limited changes in the emission spectra (Figures S10 and S11). These results are consistent with the poor excimer band formation observed in the unstrained samples: if excimers and aggregates are only barely present in the sample, we cannot expect relevant mechanochromism based on spectral variations.

In SEBS-P 5% (Figure 3a, spectra normalized on the monomeric emission), the excimer band is clearly present in the unstrained sample, and we observed a significant mechanochromism during deformation, even though only starting from 200% of strain. Drops of excimer content of around 11 and 33% were observed at 200 and 400% of strain, respectively. In the sample comprising 10 wt % of dispersed pyrene (Figure 3b, spectra normalized on the monomeric emission), the emission spectrum is characterized by the presence of almost only the excimer band, and a signal ascribable to the monomeric band started to appear during the deformation already from 50% strain onward. However, the excimer band remained dominant in the whole deformation range explored. In this case, a drop of excimer content of around 34 and 79% can be estimated at 50 and 400% of strain, respectively. In the case of the covalently functionalized SEBS-AMP sample (Figure 3c), the excimer band decreases upon deformation and the drop of excimer is already evident at 50% of strain. The excimer to monomer emission ratio changed by 30 and 78% applying 50 and 400% of strain, respectively.

The covalently functionalized system shows an improved mechanochromic response with respect to the corresponding blend doped with 1 wt % of pyrene. Ultimately, the mechanochromic properties of SEBS-AMP were similar in amplitude and in the slope of the response to those of SEBS-P 10%, which contains about 10 times the amount of pyrene molecules. This can be explained on the basis that in the former, the pyrenic units are confined within the ethylene−butylene soft block of the polymeric matrix, thus resulting in a higher local concentration leading to increased excimer formation. Yet, the enhanced response and sensitivity to applied stress are not a mere effect of concentration. The amorphous soft block grants the elastic properties to the matrix; therefore, fluorophores are strategically localized in the phase that bears the earliest mechanical stress, resulting in a more efficient breakage of the


https://doi.org/10.1021/acsapm.2c02037
ACS Appl. Polym. Mater. 2023, 5, 1545−1555

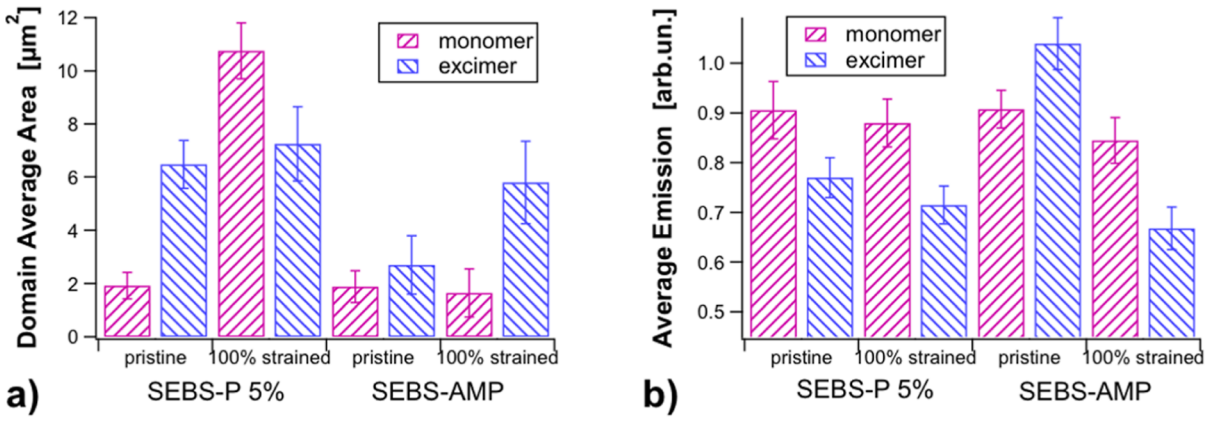


**Figure 5.** Average area of the emission domains in SEBS-P 5% and SEBS-AMP samples before and after stretching (a) and corresponding average emission intensity (b).

aggregates during deformation, an enhanced mechanochromic response, and an improved sensitivity toward the applied force. In other words, the covalent functionalization of the ethylene−butylene soft block allowed the formation of (possibly smaller) pyrene excimers, which appeared, however, more responsive than the mixed 5 wt %. The mechanochromic response in the blend films required larger amounts of pyrene since it can be preferentially incorporated in the polystyrene blocks that are less active during the uniaxial solicitation. A deeper analysis is given in Section 3.3. Since SEBS-P 10% and SEBS-AMP showed the best $I_E/I_M$ variation between pristine and 400% stress (−79 and −78%, respectively), these samples were further characterized to investigate the reversibility of the mechanochromic response. To this aim, the films were tested under successive cycles of strain (up to 400%, Figure 3d,e). The $I_E/I_M$ values remained within 10% of their initial values across 5 cycles for both systems. These experiments show that the hard phase of the styrene blocks acts effectively as anchor points for the macromolecular chains in both SEBS-P 10% (Figure 3d) and SEBS-AMP (Figure 3e) samples, leading to reversible deformation and reversible mechanochromic response.

For a more detailed comparison of SEBS-P 10% and SEBS-AMP, Figure 4 shows the results of time-resolved emission measurements after film deformation at different predefined strains. More in detail, Figure 4a,b report, for each sample, the emission decay of the monomer (measured at 398 nm) at different strains. It is evident that these emission decays can be divided into a long component (which is actually made of two contributions, one at about 25 ns and one at ca. 130−170 ns, matching the expected monomeric pyrene decays in the presence and in the absence of oxygen as a quencher, respectively) which represents the unquenched monomeric pyrene moieties; the other contribution is instead characterized by a short decay (0.6−3 ns) that accounts for those pyrene moieties involved in the formation of excimers and aggregates with a distribution of quenching rates—owing to different pyrene−pyrene distances. These two fractions are quantified by a three-exponential fitting and by plotting the two pre-exponential coefficients. After a preliminary fitting, 3 fixed lifetimes (2, 25, and 130 ns for the SEBS-AMP and 1, 25, and 170 ns for the SEBS-P 10%) were selected to optimize the quantification of pre-exponential factor contributions. Since the pyrene moieties feature the same radiative constants, these coefficients can be regarded as roughly proportional to the molar fraction of pyrene moieties which are involved in excimer formation (B1) with respect to the monomers that are not involved in the excimer formation (B2 + B3). Notably, with the increase of strain, the fraction of excimer-forming pyrene moieties decreases and, concomitantly, the fraction of unquenched pyrene monomers increases. In SEBS-AMP, i.e., in the presence of covalently bound pyrene, this transition appears to be sharper and to involve a larger fraction of pyrene moieties, with respect to what observed in SEBS doped with 10 wt % of physically dispersed pyrene.

**3.3. Characterization by SNOM.** A relevant aspect concerns the spatial distribution of the emission at the sample surface. To get useful insight in this direction, SNOM on SEBS-AMP, SEBS-P 5%, and SEBS-P −10% was performed to evaluate the morphological features before and after 100% of strain and near-field operation assessed as in Figure S15. The fluorescence emission, stimulated in the near-field at 365 nm and collected in the far-field, was split and sent onto two separate detectors equipped with interference filters centered at 405 and 458 nm (bandwidth 10 nm), respectively. In this way, maps representative of the spatial distribution of monomer and excimer emission, respectively, were simultaneously acquired. The emission maps acquired on pristine and strained SEBS-P 10% film turned out almost homogeneous, possibly because of the strong excimer emission that saturated the signal collected by the analysis. Therefore, this sample was not further investigated. Figure S16 shows examples of the so-realized maps acquired during 4 $\mu$m × 4 $\mu$m scans on both pristine and strained SEBS-P 5% and SEBS-AMP samples. In addition to the emission maps, we also included the topographies reconstructed during the same scans. Inhomogeneous topographical features were detected, possibly affected by surface irregularities in the mold. Roughness analysis conducted on SEBS-P 5% and SEBS-AMP topographies resulted in a root-mean-square roughness ($S_q$) of 20 ± 4 and 27 ± 6 nm, respectively. The uniaxial deformation, oriented approximately along the diagonal of the images, produced an increase in roughness due to the formation of elongated structures in the stretching direction, clearly visible in the maps (Figure S16). For the strained SEBS-P 5% sample, $S_q$ was found to be 41 ± 9 nm; for the SEBS-AMP sample, $S_q$ was 36 ± 12 nm. Although generally correlated with topography, emission maps exhibit qualitatively different morphologies. For the excimer band, emission domains, i.e., regions where the emission intensity is almost homogeneous, extend over relatively large areas (typical of a few $\mu$m). By contrast, the emission of the monomer is more spatially dispersed and granular, featuring


https://doi.org/10.1021/acsapm.2c02037
ACS Appl. Polym. Mater. 2023, 5, 1545−1555

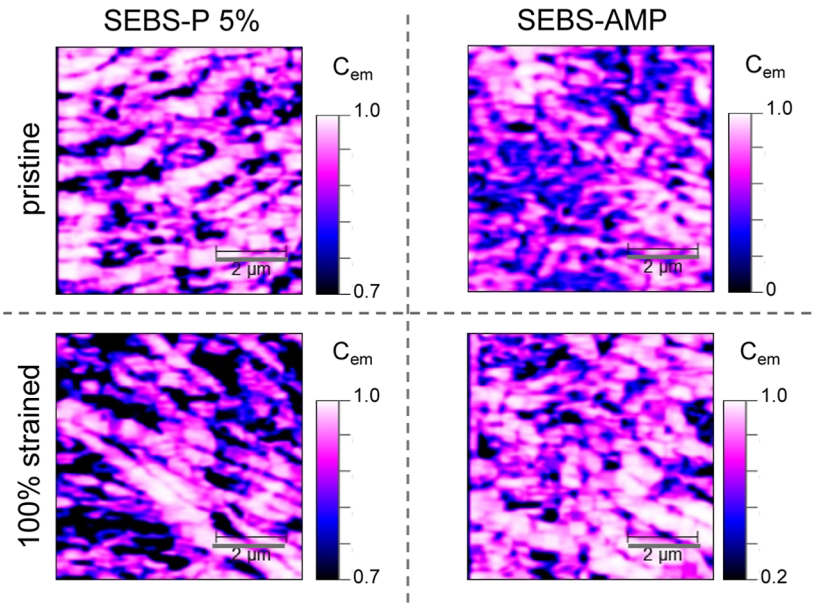


**Figure 6.** Excimer/monomer correlation maps for SEBS-P 5% and SEBS-AMP samples. Scale bar = 2 $\mu$m.

submicrometric domains appearing, in particular, in the SEBS-AMP sample. In near-field scans, only the outmost layers are subjected to excitation since the near-field extinguishes on a length scale of a few tens of nanometers. Therefore, the finding can be ascribed to the uneven spatial distribution of the pyrene units at the sample surface, possibly leading to the granular morphology of monomer emission maps. Conversely, agglomeration involved in the excimer formation occurs on a larger length scale, giving rise to more extended and homogeneous domains.

According to this analysis, strain induces changes in the morphology of PL domains. In particular, in the PL maps of the excimer, domains of typically 1−2 $\mu$m width and elongated shape along the stretching direction are clearly visible. For their size and shape, they are comparable to topographic structures. Similar elongated domains in the stretching direction are also observed in the case of the monomer, despite being more finely divided, as mentioned earlier. A standard cell-counting algorithm, based on the Otsu method (Figure S17), has been applied to the whole set of emission maps produced in the experiment, corresponding to a total scanned area of about 200 $\mu m^2$ per sample. This enabled determining an average area of the emission domains in different samples and strain conditions (Figure 5a). They confirm the granular distribution of the monomer emission domains that, in fact, show in most samples an average smaller area than the excimer ones. There is, however, a notable exception for the strained SEBS-P 5% sample, where maps suggested an increase of the monomer domain area by a factor ca. 5 upon application of the mechanical strain. We note that, conversely, the average emission intensity calculated on the same maps, summarized in Figure 5b, did not increase with respect to the pristine conditions. This means that, rather than modifying the monomer/excimer intensity ratio, strain led to an improved homogeneity of the monomer distribution at the sample surface driven by mechanical stress. This is in line with the constant monomer/excimer intensity ratio recorded by emission spectroscopy for the SEBS-P 5% sample at 100% strain, as reported in Figure 3a.

The marked mechanochromism of SEBS-AMP is also confirmed in near-field investigations. As shown in Figure 5b, mechanical strain promotes a decrease in the average intensity of the excimer emission, in substantial agreement with the macroscopic fluorescence measurements. This is accompanied by an increase in the grain area by a factor of about 3, suggesting that, upon strain, the surviving excimer species reorganize their spatial distribution within wider domains at the sample surface. The behavior is, therefore, similar to that of the monomer species in the dispersed material. However, we can hypothesize a slightly different mechanism, where, on the one hand, the mechanical stress acts to distribute over larger areas the pyrene units are covalently linked to the polymer matrix, while, on the other hand, it promotes efficient segregation of aggregates.

In addition, we evaluated the morphological correlation between the spatial distribution of excimer and monomer domains (Figure 6). As detailed in the Supporting Information (eqs S1−S3), cross-correlation ($C_{em}$) is a term used to describe the distribution of different variables in a set and can have values between 1 and −1, with 1 and −1 describing an interdependence of the variables and 0 representing a random relation between the two. In the case presented herein, $C_{em}$ between excimer and monomer emission intensities was always found to be positive. This result indicates that the local trends of the intensities are similar and may be interpreted assuming a similar spatial distribution of the dye (in the monomeric and aggregated forms) on the surface of the samples. In both SEBS-P 5% and SEBS-AMP, the application of a strain resulted in features roughly aligned with the uniaxial deformation, confirming that mechanical stress effectively drives the dye's spatial distribution. There are, however, qualitative differences in the investigated samples. First of all, in SEBS-P 5%, cross-correlation is higher, on average, with respect to SEBS-AMP, as demonstrated by the color scale range in Figure 6. This means that spatial distributions of monomer and excimer emission domains are similar to each other, being substantially ruled by the local surface density of the dispersed dye molecules. In this case, mechanical stress induces a spatial rearrangement of such density. On the contrary, when the dye is covalently linked to the polymer matrix, regions exist at the sample surface where the emission of the excimer, detected in the scan, is poorly correlated with that of the monomer and vice-versa. Although


https://doi.org/10.1021/acsapm.2c02037
ACS Appl. Polym. Mater. 2023, 5, 1545−1555

with the limitations inherently related to the finite spatial resolution of the technique (the minimum transverse size of the features observed in cross-correlation maps is on the order of 100 nm, or slightly smaller), this result may be interpreted as the evidence of a different spatial distribution of the dye molecules accompanied with a possibly increased local density of pyrene molecules, hence an enhanced probability of aggregation. In such conditions, the applied mechanical stress promotes molecular segregation, leading to a slight increase in the cross-correlation due to the co-location of monomer and excimer domains, meaning that the strain had the effect of converting part of the excimers into monomers, thus confirming the emission results. Moreover, as mentioned earlier, the spatial distribution of the surviving aggregates becomes more homogeneous.

## 4. CONCLUSIONS

In this work, two different procedures were proposed for the preparation of SEBS elastomers endowed with mechanochromic properties. The covalent approach provided ∼1 wt % of pyrene molecules grafted on the flexible ethylene−butylene blocks of SEBS (SEBS-AMP), which was compared with the physical dispersion of blend films containing variable pyrene contents, i.e., from 1 to 10 wt % (SEBS-P 1−10%). Both procedures did not substantially affect the mechanical and thermal behaviors of the derived films. Spectroscopic and SNOM investigations evidenced a modest chromogenic response under uniaxial stress for the blend films up to 5 wt % of pyrene content, possibly due to the insufficient formation of pyrene excimers. Conversely, SEBS-AMP displayed an evident pyrene excimer band at about 480 nm, possibly caused by the strategic confinement of the pyrene chromophores in the soft block of SEBS. The larger mobility of the aliphatic phase, which thus also bears most of the mechanical stress, causes an early and noticeable drop of the $I_E/I_M$ ratio and a marked mechanochromism already at 50% of strain due to the (reversible) rupture of the pyrene excimers. A similar chromogenic response occurred in blend films containing dispersed 10 wt % of pyrene. Such a high concentration was required—in the physically dispersed blend—for the formation of a responsive excimer band, probably due to a favorable solubility of pyrene and also in the styrene blocks of SEBS. For this reason, notwithstanding the clear decrease in the $I_E/I_M$ ratio, the excimer emission remained predominant up to the greatest deformation. These results highlight the significant potential for low-cost materials based on widely used commodity elastomers capable of showing reversible mechanochromic response. There is no doubt that the physical mixing offers a simpler route in gathering mechanochromism, but the optimization of the $I_E/I_M$ ratio seems less straightforward. Conversely, the covalent approach presents high potentialities and some advantages, especially when the probe is confined in a segregated domain. Modest amounts of the chromogenic probe are actually required for the emersion of the excimer band, thus allowing better control of the aggregation/de-aggregation process and a complete chromogenic effect.

## ASSOCIATED CONTENT

### Supporting Information

The Supporting Information is available free of charge at https://pubs.acs.org/doi/10.1021/acsapm.2c02037.

Additional characterization details including $^1$H NMR, FTIR, and UV−vis spectra, thermal and mechanical analysis, fluorescence, and SNOM experiments (PDF)

## AUTHOR INFORMATION


### Corresponding Author

**Andrea Pucci** − *Department of Chemistry and Industrial Chemistry and INSTM UdR of Pisa, University of Pisa, 56124 Pisa, Italy;* orcid.org/0000-0003-1278-5004; Phone: +390502219270; Email: andrea.pucci@unipi.it

### Authors

**Cosimo Micheletti** − *Department of Chemistry and Industrial Chemistry and INSTM UdR of Pisa, University of Pisa, 56124 Pisa, Italy*

**Valentina Antonia Dini** − *Department of Chemistry "Giacomo Ciamician" and INSTM UdR of Bologna, University of Bologna, 40126 Bologna, Italy*

**Marco Carlotti** − *Department of Chemistry and Industrial Chemistry and INSTM UdR of Pisa, University of Pisa, 56124 Pisa, Italy*

**Francesco Fuso** − *Department of Physics, University of Pisa, I-56127 Pisa, Italy;* orcid.org/0000-0003-2020-7343

**Damiano Genovese** − *Department of Chemistry "Giacomo Ciamician" and INSTM UdR of Bologna, University of Bologna, 40126 Bologna, Italy;* orcid.org/0000-0002-4389-7247

**Nelsi Zaccheroni** − *Department of Chemistry "Giacomo Ciamician" and INSTM UdR of Bologna, University of Bologna, 40126 Bologna, Italy*

**Chiara Gualandi** − *Department of Chemistry "Giacomo Ciamician" and INSTM UdR of Bologna, University of Bologna, 40126 Bologna, Italy;* orcid.org/0000-0002-2020-1892

Complete contact information is available at: https://pubs.acs.org/10.1021/acsapm.2c02037


### Notes

The authors declare no competing financial interest.

## ACKNOWLEDGMENTS

This work was supported by the MIUR-PRIN 20179BJNA2. Open access funding provided by University of Pisa within the CRUI-CARE Agreement.

## REFERENCES


(1) Beyer, M. K.; Clausen-Schaumann, H. Mechanochemistry: The Mechanical Activation of Covalent Bonds. *Chem. Rev.* **2005**, *105*, 2921−2948.

(2) Caruso, M. M.; Davis, D. A.; Shen, Q.; Odom, S. A.; Sottos, N. R.; White, S. R.; Moore, J. S. Mechanically-Induced Chemical Changes in Polymeric Materials. *Chem. Rev.* **2009**, *109*, 5755−5798.

(3) Simon, Y. C.; Craig, S. L. *Mechanochemistry in Materials*; Simon, Y. C., Craig, S. L., Eds.; *Polymer Chemistry Series*; Royal Society of Chemistry: Cambridge, U.K., 2017. DOI: 10.1039/9781782623885.

(4) Callister, W. D.; Rethwisch, D. G. *Fundamentals of Materials Science and Engineering: An Integrated Approach*, 3th ed.; Wiley: Hoboken, NJ, 2007

(5) Roberts, D. R. T.; Holder, S. J. Mechanochromic Systems for the Detection of Stress, Strain and Deformation in Polymeric Materials. *J. Mater. Chem.* **2011**, *21*, 8256−8268.

(6) Deneke, N.; Rencheck, M. L.; Davis, C. S. An Engineer's Introduction to Mechanophores. *Soft Matter* **2020**, *16*, 6230−6252.

(7) Patrick, J. F.; Robb, M. J.; Sottos, N. R.; Moore, J. S.; White, S. R. Polymers with Autonomous Life-Cycle Control. *Nature* **2016**, *540*, 363−370.
(8) Chen, Y.; Mellot, G.; van Luijk, D.; Creton, C.; Sijbesma, R. P. Mechanochemical Tools for Polymer Materials. *Chem. Soc. Rev.* **2021**, *50*, 4100−4140.
(9) O'Neill, R. T.; Boulatov, R. The Many Flavours of Mechanochemistry and Its Plausible Conceptual Underpinnings. *Nat. Rev. Chem.* **2021**, *5*, 148−167.
(10) Brantley, J. N.; Wiggins, K. M.; Bielawski, C. W. Polymer Mechanochemistry: The Design and Study of Mechanophores. *Polym. Int.* **2013**, *62*, 2−12.
(11) Binder, W. H. The "Labile" Chemical Bond: A Perspective on Mechanochemistry in Polymers. *Polymer* **2020**, *202*, 122639.
(12) Li, J.; Nagamani, C.; Moore, J. S. Polymer Mechanochemistry: From Destructive to Productive. *Acc. Chem. Res.* **2015**, *48*, 2181−2190.
(13) Traeger, H.; Kiebala, D. J.; Weder, C.; Schrettl, S. From Molecules to Polymers—Harnessing Inter- and Intramolecular Interactions to Create Mechanochromic Materials. *Macromol. Rapid Commun.* **2021**, *42*, 2000573.
(14) He, S.; Stratigaki, M.; Centeno, S. P.; Dreuw, A.; Göstl, R. Tailoring the Properties of Optical Force Probes for Polymer Mechanochemistry. *Chem. - Eur. J.* **2021**, *27*, 15889−15897.
(15) Kim, T. A.; Beiermann, B. A.; White, S. R.; Sottos, N. R. Effect of Mechanical Stress on Spiropyran-Merocyanine Reaction Kinetics in a Thermoplastic Polymer. *ACS Macro Lett.* **2016**, *5*, 1312−1316.
(16) Lee, C. K.; Beiermann, B. A.; Silberstein, M. N.; Wang, J.; Moore, J. S.; Sottos, N. R.; Braun, P. V. Exploiting Force Sensitive Spiropyrans as Molecular Level Probes. *Macromolecules* **2013**, *46*, 3746−3752.
(17) Lee, C. K.; Davis, D. A.; White, S. R.; Moore, J. S.; Sottos, N. R.; Braun, P. V. Force-Induced Redistribution of a Chemical Equilibrium. *J. Am. Chem. Soc.* **2010**, *132*, 16107−16111.
(18) Raisch, M.; Genovese, D.; Zaccheroni, N.; Schmidt, S. B.; Focarete, M. L.; Sommer, M.; Gualandi, C. Highly Sensitive, Anisotropic, and Reversible Stress/Strain-Sensors from Mechanochromic Nanofiber Composites. *Adv. Mater.* **2018**, *30*, 1802813.
(19) Yuan, W.; Yuan, Y.; Yang, F.; Wu, M.; Chen, Y. Improving Mechanoluminescent Sensitivity of 1,2-Dioxetane-Containing Thermoplastic Polyurethanes by Controlling Energy Transfer across Polymer Chains. *Macromolecules* **2018**, *51*, 9019−9025.
(20) Yan, C.; Yang, F.; Wu, M.; Yuan, Y.; Chen, F.; Chen, Y. Phase-Locked Dynamic and Mechanoresponsive Bonds Design toward Robust and Mechanoluminescent Self-Healing Polyurethanes: A Microscopic View of Self-Healing Behaviors. *Macromolecules* **2019**, *52*, 9376−9382.
(21) Chen, Y.; Sijbesma, R. P. Dioxetanes as Mechanoluminescent Probes in Thermoplastic Elastomers. *Macromolecules* **2014**, *47*, 3797−3805.
(22) Liu, S.; Yuan, Y.; Li, J.; Sun, S.; Chen, Y. An Optomechanical Study of Mechanoluminescent Elastomeric Polyurethanes with Different Hard Segments. *Polym. Chem.* **2020**, *11*, 1877−1884.
(23) Imato, K.; Irie, A.; Kosuge, T.; Ohishi, T.; Nishihara, M.; Takahara, A.; Otsuka, H. Mechanophores with a Reversible Radical System and Freezing-Induced Mechanochemistry in Polymer Solutions and Gels. *Angew. Chem., Int. Ed.* **2015**, *54*, 6168−6172.
(24) Imato, K.; Kanehara, T.; Nojima, S.; Ohishi, T.; Higaki, Y.; Takahara, A.; Otsuka, H. Repeatable Mechanochemical Activation of Dynamic Covalent Bonds in Thermoplastic Elastomers. *Chem. Commun.* **2016**, *52*, 10482−10485.
(25) Imato, K.; Kanehara, T.; Ohishi, T.; Nishihara, M.; Yajima, H.; Ito, M.; Takahara, A.; Otsuka, H. Mechanochromic Dynamic Covalent Elastomers: Quantitative Stress Evaluation and Autonomous Recovery. *ACS Macro Lett.* **2015**, *4*, 1307−1311.
(26) Pucci, A.; Bizzarri, R.; Ruggeri, G. Polymer Composites with Smart Optical Properties. *Soft Matter* **2011**, *7*, 3689−3700.
(27) Pucci, A.; Ruggeri, G. Mechanochromic Polymer Blends. *J. Mater. Chem.* **2011**, *21*, 8282−8291.
(28) Donati, F.; Pucci, A.; Cappelli, C.; Mennucci, B.; Ruggeri, G. Modulation of the Optical Response of Polyethylene Films Containing Luminescent Perylene Chromophores. *J. Phys. Chem. B* **2008**, *112*, 3668−3679.
(29) Sagara, Y.; Karman, M.; Seki, A.; Pannipara, M.; Tamaoki, N.; Weder, C. Rotaxane-Based Mechanophores Enable Polymers with Mechanically Switchable White Photoluminescence. *ACS Cent. Sci.* **2019**, *5*, 874−881.
(30) Muramatsu, T.; Sagara, Y.; Traeger, H.; Tamaoki, N.; Weder, C. Mechanoresponsive Behavior of a Polymer-Embedded Red-Light Emitting Rotaxane Mechanophore. *ACS Appl. Mater. Interfaces* **2019**, *11*, 24571−24576.
(31) Traeger, H.; Sagara, Y.; Kiebala, D. J.; Schrettl, S.; Weder, C. Folded Perylene Diimide Loops as Mechanoresponsive Motifs. *Angew. Chem., Int. Ed.* **2021**, *60*, 16191−16199.
(32) Traeger, H.; Sagara, Y.; Berrocal, J. A.; Schrettl, S.; Weder, C. Strain-Correlated Mechanochromism in Different Polyurethanes Featuring a Supramolecular Mechanophore. *Polym. Chem.* **2022**, *13*, 2860−2869.
(33) Sagara, Y.; Traeger, H.; Li, J.; Okado, Y.; Schrettl, S.; Tamaoki, N.; Weder, C. Mechanically Responsive Luminescent Polymers Based on Supramolecular Cyclophane Mechanophores. *J. Am. Chem. Soc.* **2021**, *143*, 5519−5525.
(34) Pucci, A.; Di Cuia, F.; Signori, F.; Ruggeri, G. Bis(Benzoxazolyl)-Stilbene Excimers as Temperature and Deformation Sensors for Biodegradable Poly(1,4-Butylene Succinate) Films. *J. Mater. Chem.* **2007**, *17*, 783−790.
(35) Pucci, A.; Bertoldo, M.; Bronco, S. Luminescent Bis-(Benzoxazolyl)Stilbene as a Molecular Probe for Poly(Propylene) Film Deformation. *Macromol. Rapid Commun.* **2005**, *26*, 1043−1048.
(36) Muramatsu, T.; Okado, Y.; Traeger, H.; Schrettl, S.; Tamaoki, N.; Weder, C.; Sagara, Y. Rotaxane-Based Dual Function Mechanophores Exhibiting Reversible and Irreversible Responses. *J. Am. Chem. Soc.* **2021**, *143*, 9884−9892.
(37) Löwe, C.; Weder, C. Oligo(p-Phenylene Vinylene) Excimers as Molecular Probes: Deformation-Induced Color Changes in Photoluminescent Polymer Blends. *Adv. Mater.* **2002**, *14*, 1625−1629.
(38) Crenshaw, B. R.; Burnworth, M.; Khariwala, D.; Hiltner, A.; Mather, P. T.; Simha, R.; Weder, C. Deformation-Induced Color Changes in Mechanochromic Polyethylene Blends. *Macromolecules* **2007**, *40*, 2400−2408.
(39) Crenshaw, B. R.; Weder, C. Deformation-Induced Color Changes in Melt-Processed Photoluminescent Polymer Blends. *Chem. Mater.* **2003**, *15*, 4717−4724.
(40) Crenshaw, B. R.; Weder, C. Self-Assessing Photoluminescent Polyurethanes. *Macromolecules* **2006**, *39*, 9581−9589.
(41) Cellini, F.; Block, L.; Li, J.; Khapli, S.; Peterson, S. D.; Porfiri, M. Mechanochromic Response of Pyrene Functionalized Nanocomposite Hydrogels. *Sens. Actuators, B* **2016**, *234*, 510−520.
(42) Roberts, D. R. T.; Patel, M.; Murphy, J. J.; Holder, S. J. Optical Response to Stress in Pyrene Labelled Polydimethylsiloxane Elastomers: Monitoring Strain in 1D and 2D. *Sens. Actuators, B* **2012**, *162*, 43−56.
(43) Rossi, N. A. A.; Duplock, E. J.; Meegan, J.; Roberts, D. R. T.; Murphy, J. J.; Patel, M.; Holder, S. J. Synthesis and Characterisation of Pyrene-Labelled Polydimethylsiloxane Networks: Towards the in Situ Detection of Strain in Silicone Elastomers. *J. Mater. Chem.* **2009**, *19*, 7674−7686.
(44) Rasch, D.; Göstl, R. Pyrene-Based Macrocrosslinkers with Supramolecular Mechanochromism for Elastic Deformation Sensing in Hydrogel Networks. *Org. Mater.* **2022**, *4*, 170−177.
(45) Zych, A.; Verdelli, A.; Soliman, M.; Pinalli, R.; Pedrini, A.; Vachon, J.; Dalcanale, E. Strain-Reporting Pyrene-Grafted Polyethylene. *Eur. Polym. J.* **2019**, *111*, 69−73.
(46) Winnik, F. Photophysics of Preassociated Pyrenes in Aqueous Polymer Solutions and in Other Organized Media. *Chem. Rev.* **1993**, *93*, 587−614.
(47) Basu, B. J.; Thirumurugan, A.; Dinesh, A. R.; Anandan, C.; Rajam, K. S. Optical Oxygen Sensor Coating Based on the Fluorescence Quenching of a New Pyrene Derivative. *Sens. Actuators, B* **2005**, *104*, 15−22.


https://doi.org/10.1021/acsapm.2c02037
*ACS Appl. Polym. Mater.* 2023, 5, 1545−1555

(48) Coleman, L. E.; Bork, J. F.; Dunn, H. Reaction of Primary Aliphatic Amines with Maleic Anhydride. *J. Org. Chem.* **1959**, *24*, 135−136.
(49) Hu, G. H.; Lindt, J. T. Amidification of Poly(Styrene-Co-Maleic Anhydride) with Amines in Tetrahydrofuran Solution: A Kinetic Study. *Polym. Bull.* **1992**, *29*, 357−363.
(50) Bruch, M.; Mäder, D.; Bauers, M.; Loontjens, F.; Mülhaupt, T. Melt Modification of Poly(Styrene-Co-Maleic Anhydride) with Alcohols in the Presence of 1,3-Oxazolines. *J. Polym. Sci., Part A: Polym. Chem.* **2000**, *38*, 1222−1231.
(51) van der Mee, M. A. J.; Goossens, J. G. P.; van Duin, M. Thermoreversible Covalent Crosslinking of Maleated Ethylene/Propylene Copolymers with Diols. *J. Polym. Sci., Part A: Polym. Chem.* **2008**, *46*, 1810−1825.
(52) Polgar, L. M.; van Duin, M.; Broekhuis, A. A.; Picchioni, F. Use of Diels-Alder Chemistry for Thermoreversible Cross-Linking of Rubbers: The Next Step toward Recycling of Rubber Products? *Macromolecules* **2015**, *48*, 7096−7105.
(53) Johnson, G. E. Effect of Concentration on the Fluorescence Spectra and Lifetimes of Pyrene in Polystyrene Films. *Macromolecules* **1980**, *13*, 839−844.





https://doi.org/10.1021/acsapm.2c02037
*ACS Appl. Polym. Mater.* 2023, 5, 1545−1555